УДК 621.039.58 doi.org/10.31717/2311-8253.25.1.1

V. V. Goranchuk[1], **V. I. Borysenko**[1], **V. V. Stadnik**[2], **M. M. Palamarchuk**[2], **E. M. Chalyi**[2]

[1] *Institute for Safety Problems of Nuclear Power Plants, NAS of Ukraine, 12, Lysohirska st., Kyiv, 03028, Ukraine*
[2] *Branch of SS "Scientific and Technical Center" of JSC NNEGC "Energoatom", 22-24, Hoholivska st., Kyiv, 01054, Ukraine*

Energy Deposition Analysis for VVER-1000 Core Internals

Keywords:
energy deposition,
core internals,
core baffle,
VVER-1000,
MCNP

Calculation of energy deposition in metal structures under the influence of reactor irradiation is an important task in analyzing the state of reactor pressure vessel (RPV). Correct determination of energy deposition is important for obtaining initial data for assessing: temperature fields in the RPV, radiation swelling of the RPV material, and changes in the geometry of the RPV. The article presents the results of numerical modeling in the MCNP code of the process of energy deposition formation in the VVER-1000 reactor pressure vessel. The main components of energy deposition in the core baffle were considered. The energy deposition is caused by the interaction of neutrons and gammas with the core baffle material. Since there are prompt and delayed neutrons and gammas, it is necessary to take them all into account. In the model of reactor core, the prompt neutron sources are fission neutrons. Prompt gammas are produced directly during fuel fission, as well as during the interaction of neutrons with fuel (without fission), fission products, structural materials, and coolant (moderator). Delayed neutrons and gammas are emitted during the radioactive decay of fuel fission products. The amount of delayed neutrons is insignificant (0.68% for ^{235}U), the amount of delayed gammas is already significant and commensurate with the amount of prompt fission gammas. For the production of delayed particles (neutrons, gammas, beta particles, alpha particles and positrons) in the MCNP6 code, the ACT card can be used. The ACT card of the MCNP6 code is promising for modeling the delayed gammas from the decay of radioactive fission products, but it is not suitable for this calculation because it does not work together with the NONU card. Therefore, the determination of the delayed gammas was performed using the SCALE program package. The calculation results showed that the energy deposition is almost entirely due to the interaction of gammas with the core baffle material, with the contribution of delayed fission gammas to the total energy deposition amounting to 1.4–21.1%, depending on the core baffle region. Since the contribution from delayed gammas is maximum in the area where the most energy deposition is observed — on the inner surface of the core baffle — its accounting is mandatory.

In Ukraine, most of the operating VVER-1000 power units are either in long-term operation or approaching it. In this regard, there is a need to assess the technical condition and predict the remaining service life of equipment, including core internals (CIs), taking into account radiation exposure — particularly energy deposition in the reactor core baffle — throughout the entire operational period.

Energy deposition in the CIs is not a cumulative process but is determined by the current state of the reactor core (RC) — namely, reactor power, fuel assembly (FA) burnup depth, volumetric distribution of coolant density, and the critical concentration of boric acid. Therefore, for a conservative assessment, calculations should be performed for the moments of the fuel campaign that result in the maximum energy deposition in the CIs.

The assessment of energy deposition in the core baffle was performed using the Monte Carlo method with the MCNP 6.1 computer code [1]. To date, a substantial body of verification data has been accumulated regarding the use of the MCNP code in various fields of nuclear engineering, the design of new nuclear installations, and scientific research. Analysis of this data shows that the code, in all calculation modes and with the cross-section libraries supplied with the code distribution, accurately reproduces the results of benchmark experiments, which provides confidence in the reliability of the obtained results.

An analysis of the problem of determining radiation loads on the CIs of VVER-1000 reactor, based on accumulated experience, has shown that for this type of calculation, it is not necessary to use a full-scale reactor model. It is sufficient to model in detail the RC, the core baffle, the core barrel (CB), and the water layer between the reactor pressure vessel and the CB within a 60-degree symmetry sector (see Fig. 1). Vertically, the model is bounded by the upper plate of the protective tube unit (PTU) and 15 cm from the bottom of the faceted belt.

According to [2], the simulation model must use data on the materials and geometric parameters of the modeled reactor unit. These data include the composition of materials, temperatures and densities of materials by regions, as well as the geometry of the reactor unit,

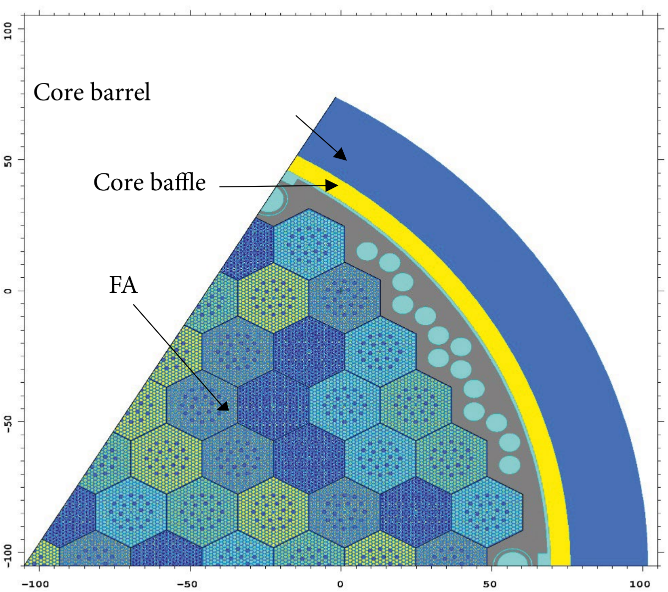

Fig. 1. Diagram of the simulation model

which comprises a detailed description of the RC, down to sub-assembly level modeling of the FAs and in-vessel components (baffle, core barrel).

The model was developed based on the following components:

reactor core;

core baffle;

PTU;

core barrel;

reactor pressure vessel.

The model includes a 60-degree sector of the RC, in which FAs with detailed geometry, including top and bottom nozzles, are modeled. In the MCNP code, the core baffle is represented as a series of rings with grooves and flanges on the outer surface, as well as a faceted inner surface that precisely replicates the external contours of the core. A corresponding gap filled with coolant is defined between the inner surface of the baffle and the outer boundary of the core. The baffle model also accounts for all vertical cooling channels, as well as horizontal and vertical grooves on its outer surface, which further enhance the cooling of the baffle material. Beyond the baffle, separated by a coolant-filled gap, CB lies. Structurally, the CB is a cylindrical shell with a flange and an elliptical bottom head.

It is evident that the sections of the core baffle and the CB located opposite the fuel region of the RC are subjected to the highest neutron irradiation. This area also corresponds to the maximum neutron fluence and energy deposition within the baffle.

The RC serves as the source of neutrons and defines the conditions for neutron transport from the point of generation to the point of detection within the model. Therefore, to accurately simulate neutron fluxes in the core baffle and CB, it is essential to model the geometry and material composition of the RC in detail, taking into account the axial variation in coolant density and fuel burnup in each FA.

When defining the neutron source for energy deposition calculations, all FAs within one-sixth of the RC were used. A sub-assembly level distribution of neutron source intensity was specified within each FA.

The isotopic composition was calculated using the ORIGEN-ARP computational sequence from the SCALE 6.1 code package [3]. The isotope composition of the spent fuel included the following 29 isotopes: ^{234}U, ^{235}U, ^{236}U, ^{238}U, ^{238}Pu, ^{239}Pu, ^{240}Pu, ^{241}Pu, ^{242}Pu, ^{147}Pm, ^{149}Pm, ^{103}Rh, ^{105}Rh, ^{147}Sm, ^{148}Sm, ^{149}Sm, ^{150}Sm, ^{151}Sm, ^{152}Sm, ^{131}Xe, ^{135}Xe, ^{135}I, ^{115}In, ^{83}Kr, ^{143}Nd, ^{145}Nd, ^{237}Np, ^{99}Tc, and ^{16}O. These isotopes saturate the full cross section of neutron interaction with matter by 98%.

In MCNP, there are two types of calculations:

criticality calculations (KCODE);

with a fixed source (SDEF).

Since the k_{eff} calculation (KCODE) involves performing successive cycles of fission (in the MCNP code, the computational equivalent of neutron generation is the k_{eff} cycle), the criticality calculation in MCNP follows a different programming logic compared to problems with a fixed source. The calculation requires a special criticality source, which is incompatible with user-defined sources. Unlike fixed source problems, where the source does not change throughout the calculation, the criticality source changes from cycle to cycle. The spatial distribution of the source for the KCODE calculation is as follows:

for the first cycle, the locations of the fission sources are taken from one of the cards — KSRC, SDEF, or SRCTP;

after the first cycle, the locations of the fission sources are taken from the previous cycle.

Energy deposition calculations in the CB were performed using a fixed neutron fission source defined in the SDEF card. Since the fission neutrons were already accounted for in the fixed source, the NONU card was used without parameters (without any entries). If the NONU card is present but without parameters, it means that all entries are set to "0", indicating that fission in all cells is treated as absorption, while gammas are still produced. Without the ability to turn off fission, performing a fixed-source calculation would not be possible due to system criticality and because the fission neutrons had already been accounted for. The use of the NONU card in non-KCODE mode allows for the correct execution of this task by treating fission as simple absorption.

To generate delayed particles (neutrons, gammas, beta particles, alpha particles, and positrons) in the MCNP6 code, the ACT card can be used. The ACT card has the following keywords: fission, nonfiss.

The fission keyword enables the generation of delayed particles from the decay of fission products that were formed as a result of fission induced by neutrons or photons. The nonfiss keyword enables the generation of delayed particles from the decay of activation products that were formed due to neutron and photon interactions (without fission). The ACT card can only be used in calculations with a fixed source.

The ACT card in MCNP6 code is a promising tool for modeling delayed gammas from fission products, but it is not suitable for this calculation because:

a critical system requires the use of the NONU card to suppress fission (which is already included in the source);

the ACT card cannot generate delayed gammas from fission products when the NONU card is used.

Therefore, the SCALE code package was used to determine the source of delayed gammas from fission products.

The energy deposition in the core baffle is primarily caused by the interaction of gammas with the atoms of the baffle material. The source of these gammas is the RC of the operating reactor. Gammas are produced as a result of nuclear interactions between neutrons and fissile isotopes (prompt gammas), as well as emitted by radioactive fission products (delayed gammas). There are three main mechanisms of energy deposition during the interaction of gammas with matter: the photoelectric effect, Compton scattering (Compton effect), and electron-positron pair production. As a result of these three fundamental mechanisms, the energy of the primary gamma is partially or completely transferred to atomic electrons, which then lose energy through ionization and radioactive deceleration. This process transfers kinetic energy to the crystalline lattice of the material, leading to heating of the material.

MCNP provides several options for calculation (registration) of flux-related quantities relevant to energy deposition calculations, including the F4 (with FM card), F6, and F7 cards [1]. The F4 card registers the neutron flux density, and when used in combination with the FM card, it can calculate the fission reaction rate as well as the energy deposition in a cell based on the number of fission events. The F6 card estimates energy deposition based on particle track length:

$$H_t = \frac{\rho_a}{m} \int dE \int dt \int dV \int d\Omega \sigma_t(E) H(E) \psi(\vec{r}, \widehat{\Omega}, E, t), \quad (1)$$

where $H_t \left[\frac{\text{MeV}}{\text{g}}\right]$ is total energy deposition in the cell, $\rho_a \left[\frac{\text{atom}}{\text{barn} \cdot \text{cm}}\right]$ is atomic density, m [g] is mass of the cell, σ_t [barn] is microscopic total cross section, $\psi(\vec{r}, \widehat{\Omega}, E, t) \left[\frac{\text{particles}}{\text{cm}^2 \cdot \text{shake} \cdot \text{MeV} \cdot \text{steradian}}\right]$ is angular flux, $H(E) \left[\frac{\text{MeV}}{\text{collision}}\right]$ is heating number, which represents the amount of energy deposited in interactions, and is defined separately for neutrons and gammas in formulas (2) and (3):

$$H_n(E) = E - \sum_i p_{i,n}(E)\left[\bar{E}_{i,n\_out}(E) + \bar{E}_{i,\gamma\_out}(E) - Q_i\right], \quad (2)$$

$H_n(E) \left[\frac{\text{MeV}}{\text{collision}}\right]$ is heating number for neutrons,

$p_{i,n}(E)$ is probability of reaction occurring upon collision with a neutron of energy E,

$\bar{E}_{i,n\_out}(E)$ [MeV] is average kinetic energy of outgoing neutrons for reaction when the incident neutron has kinetic energy E,

$\bar{E}_{i,\gamma\_out}(E)$ [MeV] is average kinetic energy of emitted gammas for reaction with an incident neutron of energy E,

Q_i [MeV] is energy release (or: heat, thermal effect) of reaction (the Q-value represents the change in rest energy of the nuclei and all particles involved in the interaction, and is defined as the difference in rest mass before and after the reaction, $Q = \Delta m \cdot c^2$, Δm where is the mass difference, and is the speed of light).

$$H_\gamma(E) = E - \sum_{i=1}^{3} p_{i,\gamma}(E)\left[\bar{E}_{i,\gamma\_out}(E)\right], \quad (3)$$

$H_\gamma(E)$ $\left[\frac{\text{MeV}}{\text{collision}}\right]$ is heating number for gammas,

$p_{i,\gamma}(E)$ is probability of reaction upon collision with a gamma of energy E,

$\bar{E}_{i,n\_out}(E)$ [MeV] is average energy of the outgoing γ-radiation for reaction upon incident gamma with energy E,

$i = 1$ is incoherent (Compton) scattering,

$i = 2$ is pair production; $\bar{E}_{i,out}(E) = 2m_0c^2 = 1.022016$ MeV (where m_0c^2 is the electron rest energy),

$i = 3$ is photoelectric absorption $\bar{E}_{i,out}(E) = 0$.

The F7 card estimates the energy deposition during fission based on the particle track length as follows:

$$H_f = \frac{\rho_a}{m} Q \int dE \int dt \int dV \int d\Omega \sigma_f(E) \psi(\vec{r}, \widehat{\Omega}, E, t), \quad (4)$$

where H_f $\left[\frac{\text{MeV}}{\text{g}}\right]$ is total energy deposition in the cell during fission, σ_f [barn] is fission cross-section, Q [MeV] is energy released per fission event, the remaining parameters are the same as in equation (1).

To collect energy deposition data, the energy tally + F6 was used, which accumulates information on all energy losses by all particles within the specified geometric regions of the model. To separately evaluate the contributions from neutrons and gammas, the tally cards F6: n and F6: p were used, respectively. The baffle was divided into elementary cells, within which data on total energy losses were collected.

The components of energy deposition that were taken into account include:

energy deposition from gammas (prompt) produced as a result of fuel fission;

energy deposition from gammas (prompt) produced during the interaction of neutrons with fuel material without fission, as well as with fission products;

energy deposition from gammas (delayed) emitted by radioactive fission products;

energy deposition from gammas (prompt) produced during the interaction of neutrons with baffle material in (n, γ) reactions;

energy deposition from gammas (prompt) produced during the interaction of neutrons with baffle material without (n, γ) reactions;

energy deposition from gammas (prompt) produced as a result of the interaction of neutrons with materials in the fuel rod cladding, guide channels, central tube, and coolant.

As a result of the assessment, the energy deposition profile in the baffle was obtained (see Fig. 2), which included contributions from both neutrons and gammas. The highest energy deposition for the considered loading occurs at the central tooth of the baffle (located at a 30° angle in Fig. 1), while the lowest energy deposition is observed on the outer surface of the baffle. The ratio of maximum to minimum energy deposition is approximately 20 times in the horizontal section.

The energy deposition from fission neutrons is negligible, accounting for a maximum of approximately 3.3% on the inner surface of the baffle (see Fig. 3).

The energy deposition is almost entirely due to the interaction of gammas with the baffle material, accounting for 96.7% to 99.3% of the total energy deposition, depending on the area of the baffle (see Fig. 4). Together, the energy deposition data from Figs. 3 and 4 form 100% of the total energy deposition.

The energy deposition from delayed gammas (produced from fission) can account for a maximum of approximately 21.7% of all gammas, with the highest contribution observed in the area of maximum energy deposition in the baffle — on the inner surface (see Fig. 5). This necessitates their mandatory inclusion in the calculations of energy deposition in the baffle.

The contribution to energy deposition from prompt gammas relative to all gammas is maximal on the outer surface of the baffle, reaching up to 98.6% (see Fig. 6). Together, the energy deposition data from Figs. 5 and 6 form 100% of the total energy deposition.

Up to 71.6% of the energy deposition from all gammas is due to gammas that were produced within the fuel (see Fig. 7):

prompt, during fission;

delayed, due to radioactive decay of fission products;

prompt, during neutron interaction with fuel but without fission.

The components of energy deposition from prompt gammas are shown in Figs. 8–12. Energy deposition in Figs. 8–10 together accounts for 100% of the total energy

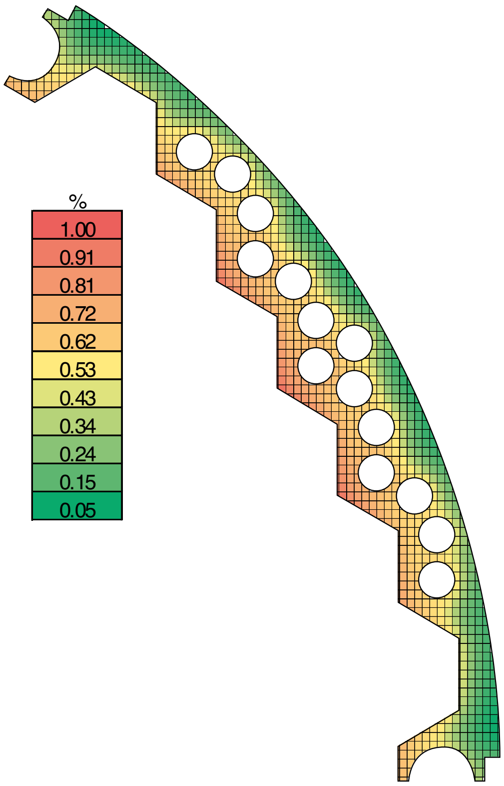

Fig. 2. Profile of energy deposition in the core baffle

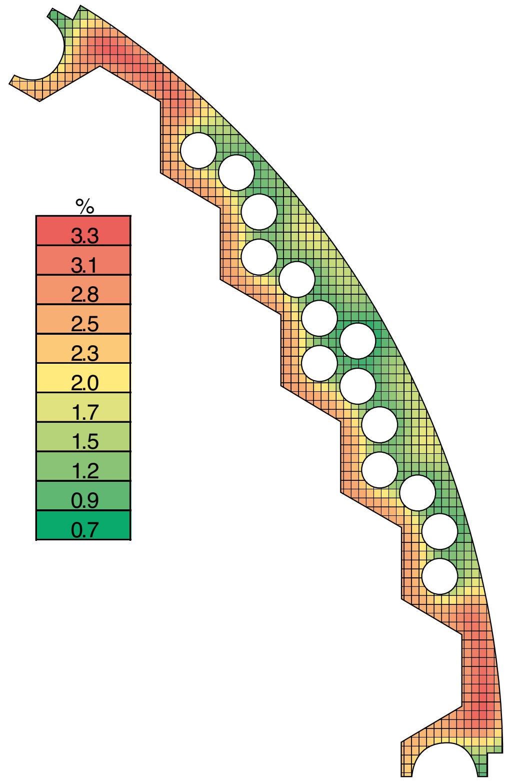

Fig. 3. The ratio of energy deposition from fission neutrons to total energy deposition, %

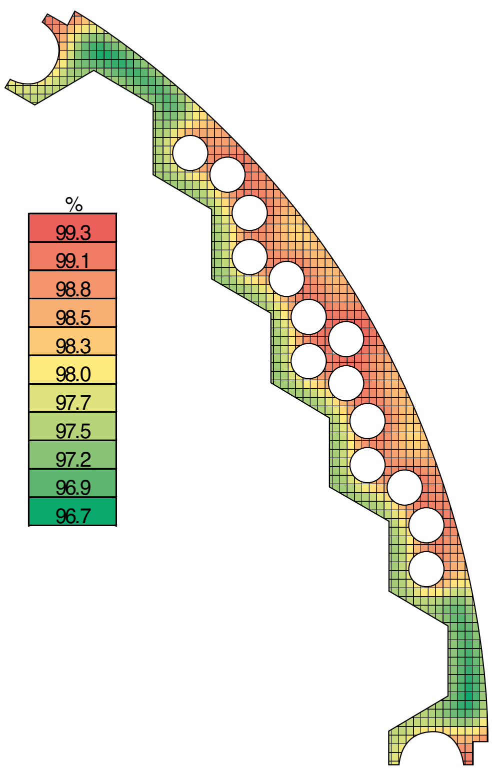

Fig. 4. Ratio of energy deposition from gammas to total energy deposition, %

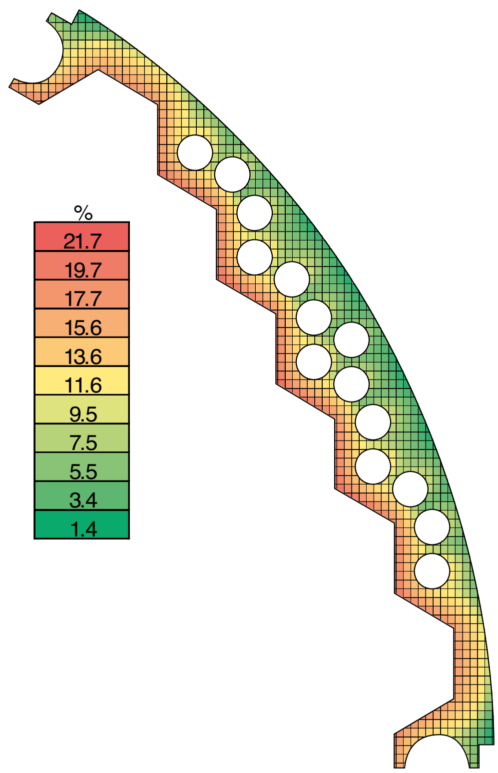

Fig. 5. Ratio of energy deposition from delayed fission gammas to total gammas, %

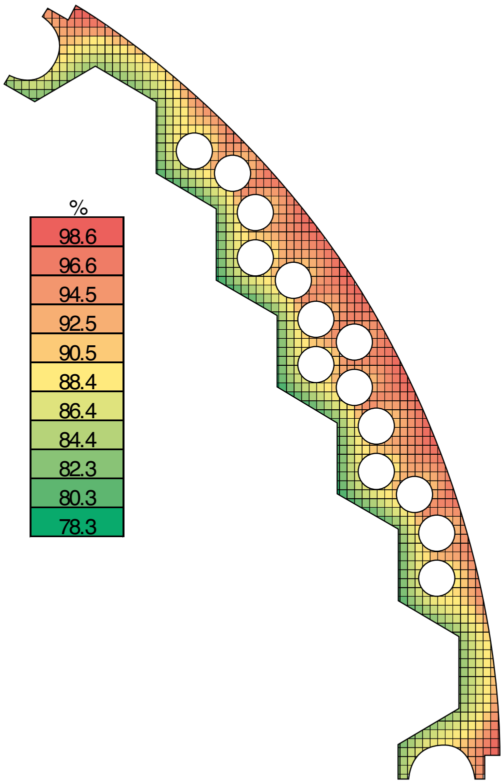

Fig. 6. Ratio of energy deposition from prompt gammas to total gammas, %

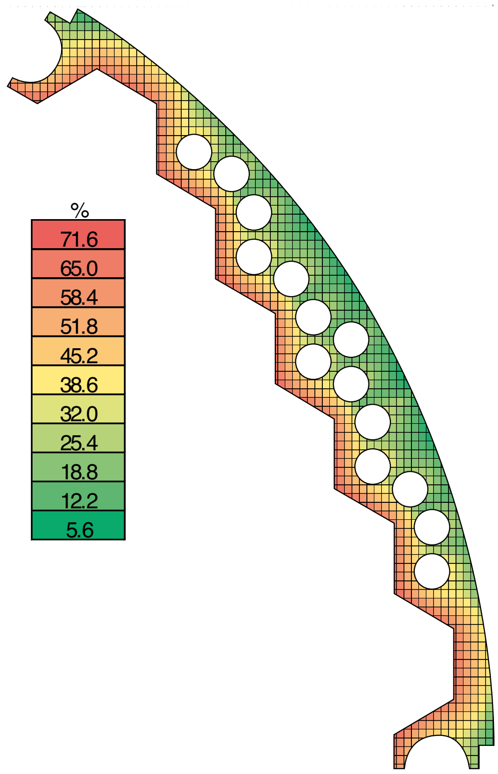

Fig. 7. Ratio of energy deposition from all gammas (prompt and delayed) generated in the fuel by neutrons to total gammas, %

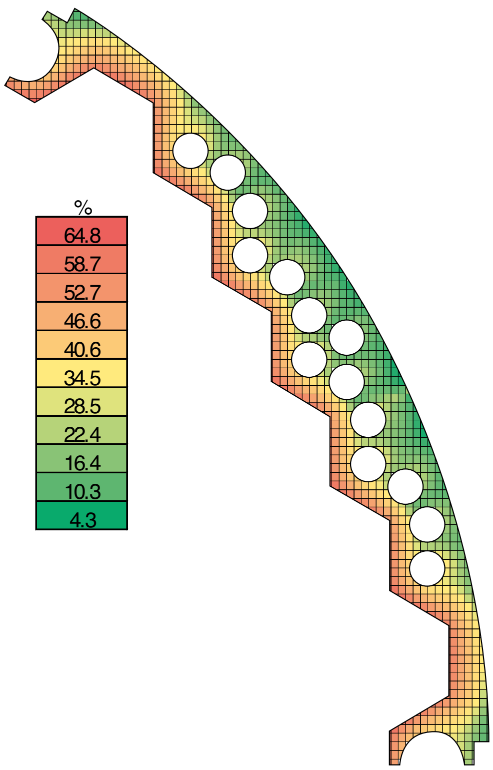

Fig. 8. Ratio of energy deposition from prompt gammas generated in the fuel by neutrons to total prompt gammas, %

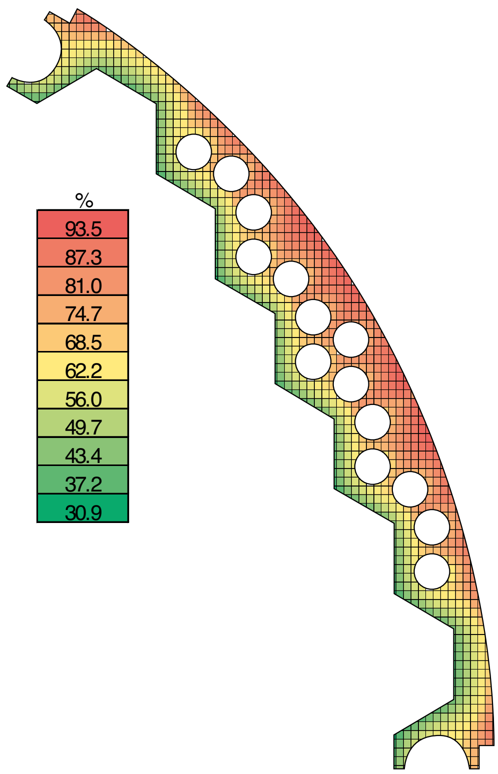

Fig. 9. Ratio of energy deposition from prompt gammas generated in the core baffle by neutrons to total prompt gammas, %

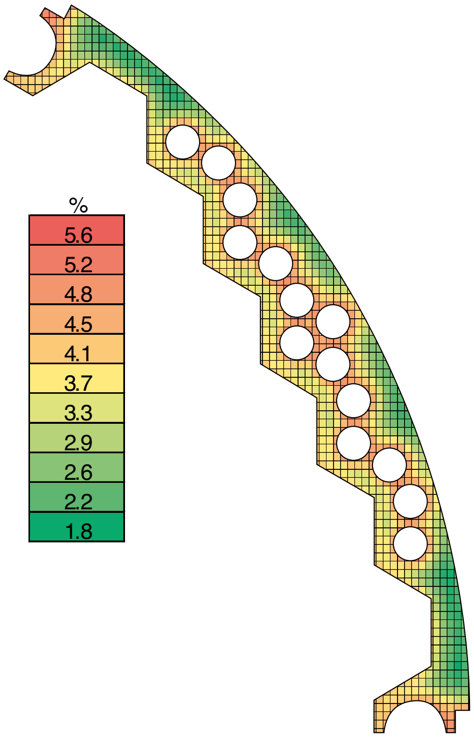

Fig. 10. Ratio of energy deposition from prompt gammas generated by neutron interactions with the materials of fuel rod cladding, guide tubes, central tube, and coolant to total prompt gammas, %

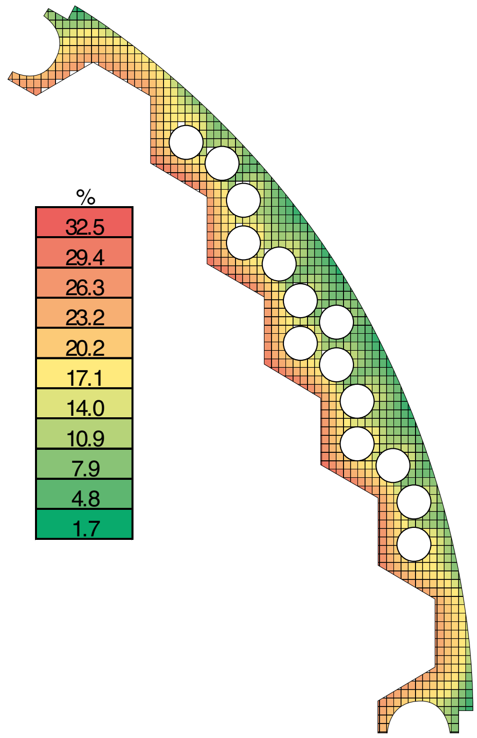

Fig. 11. Ratio of energy deposition from prompt fission gammas to total prompt gammas, %

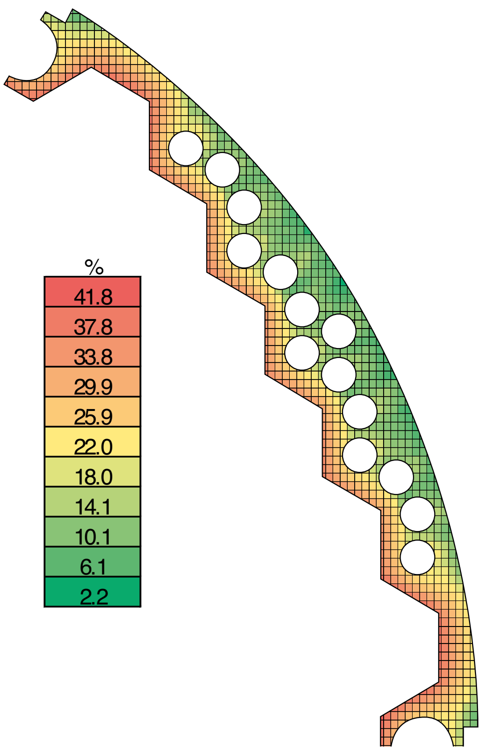

Fig. 12. Ratio of energy deposition from prompt gammas generated in the fuel by neutrons as a result of other reactions (excluding fission) to total prompt gammas, %

deposition from all prompt gammas. The energy deposition shown in Figs. 11 and 12 together forms the energy deposition represented in Fig. 8.

The correct definition of energy deposition is important for obtaining input data for the evaluation of:

temperature fields in CI.

radiation-induced swelling of the CI material.

changes in the geometry of the CI.

Conclusions

1. When calculating energy deposition in the core baffle, it is essential to account for the contribution of delayed fission gammas (1.4–21.1%, depending on the core baffle region), especially considering that this contribution is maximum in the area where the highest energy deposition is observed — on the inner surface of the core baffle.

2. The contribution of neutrons to energy deposition is negligible (0.7–3.3%, depending on the core baffle region), and for estimation (non-precise) calculations, it may be disregarded.

3. Although the direct energy deposition from neutrons is insignificant, their interaction with the core baffle metal generates secondary gammas, whose contribution to energy deposition is considerable (24.2–89.7%, depend-

ing on the core baffle region), with a maximum on the outer surface of the core baffle.

4. The energy deposition in the maximum region — on the inner surface of the core baffle — is mainly determined by gammas generated in the fuel (up to 69.7%).

References

1. MCNP6 User's Manual. Code Version 6.1., LA-CP-13-00634, May 2013.
2. Regulatory Guide 1.190 "Calculational and dosimetry methods for determining pressure vessel neutron fluence", NRC USA, March 2001.
3. Scale: A Comprehensive Modeling and Simulation Suite for Nuclear Safety Analysis and Design. ORNL/TM-2005/39, Version 6.1, June 2011.

В. В. Горанчук[1], В. І. Борисенко[1], В. В. Стаднік[2], М. М. Паламарчук[2], Е. М. Чалий[2]

[1] Інститут проблем безпеки АЕС НАН України, вул. Лисогірська 12, Київ, 03028
[2] Філія ВП «Науково-технічний центр» АТ «НАЕК "Енергоатом"», вул. Гоголівська 22-24, м. Київ, 01054

Особливості визначення енерговиділення у ВКП ВВЕР-1000

Розрахунок енерговиділення в металоконструкціях під дією реакторного опромінення є важливим завданням при аналізі стану внутрішньокорпусних пристроїв (ВКП) реактора. Коректне визначення енерговиділення важливе для отримання вихідних даних для оцінки: температурних полів у ВКП, радіаційного розпухання матеріалу та формозміни ВКП. У статті наведено результати числового моделювання в коді MCNP процесу формування енерговиділення у вигородці реактора ВВЕР-1000. Було розглянуто основні складові енерговиділення у вигородці.

Енерговиділення зумовлене взаємодією нейтронного- та γ- випромінювання з матеріалом вигородки. Оскільки складовими випромінювання є миттєві і запізнілі частинки (нейтрони і γ-кванти), то необхідно враховувати їх всіх. Джерелом миттєвих нейтронів є реакція поділу в паливі. Миттєві γ-кванти утворюються безпосередньо при діленні палива, а також при взаємодії нейтронів з паливом (без ділення), продуктами поділу, конструкційними матеріалами, теплоносієм. Запізнілі нейтрони і γ-кванти утворюються при радіоактивному розпаді продуктів поділу палива. Кількість запізнілих нейтронів є незначною (0,68 % для ^{235}U), кількість запізнілих γ-квантів вже є значною і співрозмірна з кількістю миттєвих γ-квантів поділу.

Для утворення запізнілих частинок (нейтронів, γ-квантів, бета-частинок, альфа-частинок та позитронів) в коді MCNP6 може бути використана картка ACT. Картка ACT коду MCNP6 є перспективною для моделювання запізнілих γ-квантів продуктів поділу, але не підходить для цього розрахунку оскільки разом з карткою NONU (поділ розглядається як поглинання) вона не працює. Тому визначення запізнілих γ-квантів виконувалося за допомогою пакету програм SCALE. Результати розрахунку показали, що енерговиділення майже повністю зумовлено взаємодією γ-квантів з матеріалом вигородки, при цьому внесок запізнілих γ-квантів поділу у загальне енерговиділення склав 1,4–21,1 % в залежності від розрахункової зони вигородки. Оскільки внесок від запізнілих γ-квантів максимальний в зоні, де спостерігається найбільше енерговиділення — на внутрішній поверхні вигородки — то його врахування є обов'язковим.

Ключові слова: енерговиділення, ВКП, вигородка, ВВЕР-1000, MCNP.

Надійшла / Received 09.04.2025
Рекомендована до друку / Accepted 17.04.2025